RSC Advances

ROYAL SOCIETY OF CHEMISTRY

www.rsc.org/advances

Journal Name

RSCPublishing

ARTICLE

Composite Banded Core and Non-banded Shell Transition Patterns in Stereocomplexed Poly(lactide acid) Induced by Strongly Interacting Poly(*p*-vinyl phenol)

Cite this: DOI: 10.1039/x0xx00000x

Received ooth January 2012,
Accepted ooth January 2012

DOI: 10.1039/x0xx00000x

www.rsc.org/

Hikmatun Ni'mah,[a,b] Eamor M. Woo,[a]* and Shih-Min Chang[a],

Banded core and non-banded shell with transitional patterns in stereocomplexed poly(lactic acid) sc-PLA (PLLA:PDLA=1:1) interacting with amorphous poly(*p*-vinyl phenol) (PVPh) (20-30 wt%) were investigated by using polarized optical (POM), atomic-force (AFM), and scanning electron microscopies (SEM). The center core of the spherulites is ring-banded, then transition into non-banded patterns on the outer peripheral in sc-PLA/PVPh blend crystallized at T_c=160-180°C. This composite crystal morphology is distinctly different from that of the neat sc-PLA, which is Maltese-cross without ring patterns anywhere in spherulites. The bands in the core region are also dramatically different from those bands with birefringence contrasts observed in classical ring-bands. The bands in the core show only crystal topology but no birefringence different. Both regions of ring-banded and non-banded crystals are composed of edge-on lamellae, but the central-core lamellae undergo periodical waving up and down. The specific stage-wise and preferential interactions between PVPh and sc-PLA and glass substrate, which simultaneously occur during amorphous PVPh rejection and growth process, were evaluated as some of plausible kinetic reasons for the special composite crystal morphology of sc-PLA complex induced by blending with PVPh.

Introduction

After the first finding and reporting of stereo-complexes between chiral poly(L-lactide) (PLLA) and poly(D-Lactide) (PDLA) by Ikada et al.[1], numerous studies have been conducted on the formation of the stereo-complexes as well as its crystalline morphology, crystallization behavior and physical properties.[2-4] A stereocomplexed PLA (sc-PLA) can be obtained from equi-molar (1:1) racemic mixtures of PLLA and PDLA. Physical properties of c-PLA are significantly different from those of homopolymeric PLLA or PDLA, in four aspects: (a) the melting temperature (T_m) of sc-PLA is 50°C higher than that of PLLA or PDLA,[2,5,6] (b) it crystallizes in a trigonal unit cell with 3_1-helical conformation,[7-9] (c) it is more compact and has higher mechanical properties than PLLA or PDLA,[9] and (d) unlike PLLA or PDLA, sc-PLA spherulites are not ring-banded when PDLA/PLLA blends are crystallized at any T_c. The crystalline morphology of melt-crystallized sc-PLA spherulite typically shows a Maltese-cross pattern, which may become disordered and less distinct under nonequimolar conditions, owing to less complexation extent between two chiral polymers.[1,5,10,11]

Unlike the homopolymer PLLA or PDLA that can form ring-banded spherulites at a specific crystallization condition, sc-PLA (stereo-complexed PLLA/PDLA : 1/1 mixture) has never been reported to form ring-banded spherulite at any T_c. Neat PLLA has been reported to form ring-banded spherulites at narrow range (ΔT=5°C) of T_c =125-130°C when crystallized with or without top cover.[12] However, inclusion of miscible amorphous polymers to PLLA usually does not change the ring-banding nature, but may shift the range of T_c within which ring-banded spherulites appear. PLLA can show ring-banded pattern at wider range of T_cs (110-130°C) when it was blended with poly(hydroxy butyrate) (PHB).[12] PLLA/poly(ethylene oxide) (PEO) blend melt-crystallized at T_c=110°C, at which the PEO component in the blend being in the molten amorphous state, also exhibited ring-banded pattern.[13-15] The miscible PEO component was believed to induce re-orientation of lamellae in forming ring-banded spherulites, as shown in a previous study.[16] In the miscible PEO/PLLA blends, a greater fraction of the amorphous polymer can be trapped between the lamellae of spherulites to form interference rings. On the other hand, PDLA has less been reported to form ring-banded spherulites either in neat condition or blending with another component. A study

has reported the formation of ring-banded patterns in the blend of PDLA 75/25 poly(lactide)/poly(ethylene glycol) (PEG) films crystallized at 120 °C after annealing 1 h at 160 °C.[17] In contrast to the homopolymeric PLLA or PDLA or their blends with other polymers, the equi-molar sc-PLA has never been reported to form ring-banded spherulites even after the addition of another component. Several studies have investigated several subjects of sc-PLA blended with another polymer such as PHB,[18] poly(D,L-lactide) (PDLLA),[19] poly(methyl methacrylate) (PMMA),[20] and poly(vinyl phenol) (PVPh).[21] The addition of another polymer into sc-PLA was reported to influence the crystallization behavior[19,21] and improved the processability and thermomechanical properties of sc-PLA.[20] The crystalline morphology of stereocomplexed PLA (sc-PLA) could change from original well-rounded Maltese-cross spherulites to dendritic form after being blended with high PHB contents (50 wt.% or higher) and crystallized at high T_c (130°C or above), at which PHB was in molten state or acted as an amorphous species.[18] That study shows that the addition of amorphous species could effect some changes on the crystalline morphology of sc-PLA; but none have reported findings of banded spherulites in sc-PLA or its blends.

A previous study[21] has reported the blend of sc-PLA, from 1:1 mixture of high molecular weight PLLA (HM_w-PLLA) and PDLA, with amorphous PVPh, and pointed out that PVPh influences the crystallization behavior of sc-PLA by acting as nucleating agent instead of affecting the sc-PLA crystalline morphology, which is negative type Maltese-cross spherulites. It is generally known that, although neat PLLA or PDLA may crystallize into ring-banded spherulites within a certain T_c range, their racemic 1:1 mixture forms a stereo-complex that does not form ring-banded spherulites at any T_c. Our previous study[22] has reported the crystal morphology of LM_w-PLLA/PVPh blends, which show three types of spherulites morphology. No ring-banded morphology was observed in the LM_w-PLLA/PVPh blends, suggesting that PVPh can induce the morphology changes in different aspects. In this present study, we further demonstrated that ring-banded pattern could be induced in the stereocomplex of PLLA/PDLA mixture, as long as differential interactions (among PVPh-polymer-substrate) were created. This study used low-molecular weight PLLA (LM_w-PLLA) to mix with PDLA to get sc-PLA from equi-molar mixture of PLLA and PDLA. Then, amorphous PVPh was added in order to observe its effects on the crystalline morphology and lamellar assembly of sc-PLA. The role of PVPh addition on affecting the morphology of sc-PLA was also evaluated.

Experimental Section

Materials and preparation

Poly(L-lactide) (PLLA), with a relatively low molecular weight, was purchased from Polysciences, Inc. (USA). PLLA (code name: LM_w-PLLA) was characterized using gel permeation chromatography (GPC, Waters) to reveal M_w=11,000 g/mol (PDI=1.1). LM_w-PLLA has T_g=45.3°C and T_m=155°C measured from DSC characterization. Low-molecular-weight PLLA was used for forming stereo-complex because it has a stronger complexing capacity. Poly(D-lactide) (PDLA) was obtained from Fluka, Inc. (Switzerland), with weight-average molecular weight of 124,000 g/mol, T_g(onset) =54°C and T_m=170°C. Poly(4-vinyl phenol) (PVPh) with M_w=22,000 g/mol and T_g=148°C, was obtained from Polysciences, Inc. (USA).

Film samples of stereocomplexed PLLA/PDLA and amorphous PVPh with various weight fractions were prepared by solution blending using *p*-dioxane as solvent with concentration of 4 wt.% (film thickness = 6-9 μm). The sc-PLA was obtained from equi-molar (1:1) mixture of PLLA and PDLA, which was further blended with amorphous PVPh. Thus, in the blend of sc-PLA/PVPh (70/30), the composition of each component in the ternary composition is PLLA/PDLA/PVPh (35/35/30). A drop of the polymer solution (sc-PLA/PVPh) was deposited and uniformly spread on a micro glass slide at 45 °C and the solvent was allowed to fully evaporate in atmosphere, and dried in vacuum ovens. Prior to characterization, the dried film samples were thermally treated as the following steps: samples were heated on a hot plate at a maximum melting temperature (T_{max} = 240°C) held for t_{max}=1 min for erasing the prior crystals, then rapidly removed to another hot stage pre-set at a designated isothermal T_c=110°C (or other T_c's), for full crystallization. Such procedures ensured rapid quenching to a designated temperature for isothermal crystallization with minimum temperature lag or fluctuation. For comparison purposes, the time held at T_{max}=240°C was also varied to be different from t_{max}=1 min, such as 3 or 5 min; however, T_{max}, T_c, or other thermal treatments was kept the same.

Apparatus and procedures

A polarized optical microscopy (POM, Nikon Optiphot-2), equipped with a Nikon NFX-DX exposure and Nikon NFX-35 digital camera, and a microscopic hot stage (Linkam THMS-600 with TP-92 temperature programmer), was used to characterize the optical birefringence and crystalline morphology of the crystallized samples. POM was also used for in-situ monitoring of spherulites growth measurements. Growth rate measurements of spherulites at selected T_c's were done on a temperature-controlled microscopic hot stage with digital camera and automated software capable of monitoring/recording the in-situ images spherulites in a fixed time interval.

The glass transitions (T_g) of the blend samples were measured with a differential scanning calorimeter (Diamond DSC, Perkin-Elmer) equipped with an intracooler for sub-ambient temperature down to -70°C. For determining the T_g transition temperatures, cold-crystallization, and melting transitions of the crystallized scPLA/PVPh blend, DSC characterizations were made at a heating rate of 20 °C/min. During thermal annealing or scanning, a continuous nitrogen

flow in the DSC sample cell was maintained to ensure minimal sample degradation.

Atomic-force microscopy (AFM, diCaliber, Bruker Corp.) investigations were made in intermittent tapping mode with a silicon-tip (f_o = 70 kHz, r = 10 nm) installed. The largest scan range was 150×150μm, and the scan was kept at 0.5 Hz for the overview scan and zoom-in regions (10×10μm). AFM samples were prepared in the same thermal treatments as those for POM samples. AFM measurements were also carried out to determine the height profiles and phase images for mapping the morphology and lamellar patterns of the crystals in spherulites.

Scanning Electron Microscopy (SEM) (FEI Quanta-400F, Hillsboro, OR, USA) was performed to reveal the surface morphology of the spherulites. The film samples intended for SEM characterization in this study were prepared without top cover. Prior to the SEM characterization, the top surfaces of the exposed film samples were coated with gold by vacuum sputtering.

Results and Discussion

Phase behavior and crystalline morphology

Phase homogeneity in sc-PLA/PVPh was first investigated. Although it is known that PVPh is miscible with either PLLA or PDLA in each of binary mixtures, phase behavior in ternary PLLA/PDLA/PVPh mixtures was yet to be demonstrated. **Figure 1** shows the DSC thermograms for neat PLLA-LMw, PDLA, and ternary blend of (PLLA/PDLA)/PVPh (i.e., sc-PLA/PVPh) of several compositions with increasing PVPh contents. The sc-PLA/PVPh blends (with 10–50 wt% PVPh) show a single glass transition temperature (T_g), which increases with higher PVPh contents, as shown by black-line plots in Fig. 1. The apparently single T_g with composition dependence indicates that the ternary blends are miscible over this composition range. In addition, the high T_g of PVPh component in the blend induces a significant shift in T_g of sc-PLA to higher temperatures. The endothermic melting peak of sc-PLA/PVPh blends is found to be constant as the PVPh content increases. The endothermic peak of the blends at ca. 220°C can be assigned to melting of the stereocomplex crystallites. As shown in Fig. 1 (blue and pink-line plots), the melting peak of neat LM_w-PLLA and HM_w-PDLA are around 145°C and 170°C, respectively. These melting peaks of homopolymers PLLA and PDLA do not appear in the DSC thermograph of the sc-PLA/PVPh blends, indicating that the stereocomplex crystallites were completely generated from the equi-molar mixture of PLLA and PDLA. Although no apparent down-shift of melting peak can be found upon the addition PVPh to sc-PLA, the enthalpy of melting of sc-PLA/PVPH slightly decreases as the PVPh content increases. Furthermore, the cold-crystallization temperature of the stereocomplex PLLA/PDLA shifts to a significantly higher temperature with the PVPh contents, suggesting the interactions between scPLA and PVPh. The single T_g and up-shift of cold crystallization temperature are the typical thermal behavior for a miscible blend of sc-PLA with PVPh.

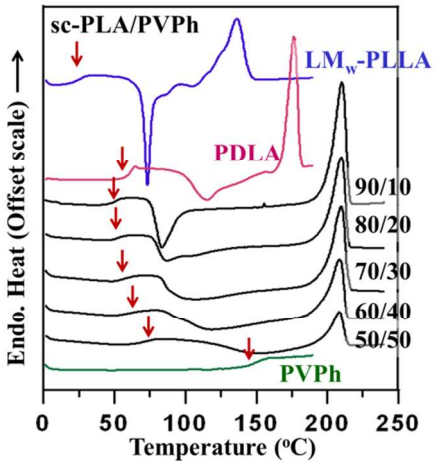

Figure 1. DSC thermograms (2nd scans) for sc-PLA/PVPh blend of different compositions as labeled on traces.

Figure 2 shows spherulites morphology of sc-PLA at various crystallization temperatures (T_c). No ring-band pattern can be observed as the T_c increases. The ringless Maltese-cross sc-PLA spherulites of LM_w-PLLA/PDLA blend exhibit negative type birefringence. The negative-type Maltese-cross spherulite found in sc-PLA is similar to the crystalline morphology of sc-PLA from equi-molar mixture of HM_w-PLLA and PDLA, as reported in a previous study,[21] which has shown that the typical crystalline morphology for neat sc-PLA is ringless and negative type when crystallized at any T_c. That is, regardless the M_w of PLLA, the spherulite patterns of scPLA are similar, although lower-M_w PLLA does have better complexing capacity with PDLA.

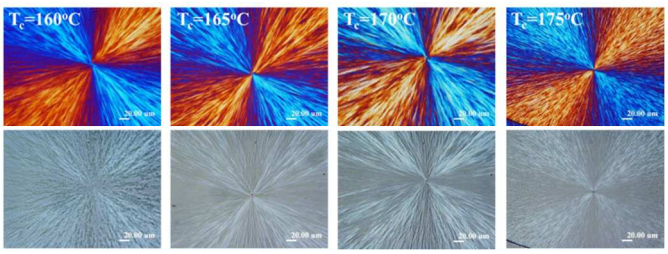

Figure 2. POM and OM images showing the crystalline morphology of neat sc-PLA at various crystallization temperatures (T_cs).

Morphology of sc-PLA blended with PVPh was compared to that of neat sc-PLA. After the addition of 30 wt.% of PVPh to sc-PLA, the crystalline morphology crystallized at a range of T_cs (160-175°C) significantly changed with the crystallization temperatures (T_cs). **Figure 3** shows POM and OM images for the crystalline morphology of sc-PLA/PVPh (70/30) blend at various crystallization temperatures (T_cs). The composite spherulites show ring-banded pattern in the central core eventually transforming into a non-banded pattern in the outer peripheral of the spherulite. The ring-band pattern in the center

of the spherulite becomes more pronounced as the T_c increases. As a matter of fact, the sizes of the banded core and width of each band steadily increase with T_c from 165 to 180°C. There are reasons that both POM and OM micrographs for crystallized sc-PLA/PVPh were characterized and discussed here. Interestingly, the bands in the central core do not show obvious birefringence differences between the ridges and valleys, in significantly opposite contrast to the obvious blue/orange birefringence colours seen in classical banded spherulites, for example. In POM images (with a tint plate), the ring-band pattern in core region is not really obvious being masked by the stronger birefringence of other dendritic crystals, however, in the OM images, the bands in the core are clear and regular enough with only crystal topology but with low or nearly non-birefringence. This fact also suggests that these ring bands in the core region of sc-PLA/PVPh may be due to only periodical height variation of the crystals but no re-orientations in the corresponding ridge/valley bands.

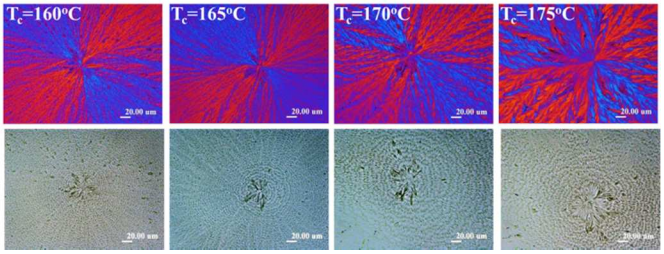

Figure 3. POM (upper row) and OM (bottom row) images showing the crystalline morphology of sc-PLA/PVPh (70/30) blend at various crystallization temperatures (T_cs=160-175°C).

Such unique and complex features with transition from banded core to non-banded outer shell in spherulites would be later further justified by AMF analysis on the central core regions. Interestingly, this special composite morphology in sc-PLA/PVPh has never been observed before in sc-PLA blends with other amorphous polymers. In present study, this unique morphology can also be seen in the sc-PLA/PVPh blend with lower PVPh content (20 wt.%), as shown in supporting evidence of Figure S1. However, the ring-banded pattern in the center region of the sc-PLA/PVPh (80/20) blend composition is less obvious than that of the sc-PLA/PVPh (70/30) blend composition. Therefore, in this present study, we chose the composition of sc-PLA/PVPh (70/30) blend melt-crystallized at T_c=170°C for further detailed characterization. When the sc-PLA was blended with smaller amount of PVPh (5 and 10 wt.%), the typical crystalline morphology of sc-PLA, with distinct Maltese-cross non-banded spherulites, did not change at all, and resemble all the features in neat sc-PLA. That is, Sc-PLA/PVPh compositions with PVPh less than 20wt.% still show negative-type Maltese-cross spherulites with no ring-band pattern, which is similar to that of neat sc-PLA.

Supporting evidence in Figure S2 shows the crystalline morphology of (a) sc-PLA/PVPh (95/5) and (b) sc-PLA/PVPh (90/10) blends at various crystallization temperatures (T_cs). From this observation, it is clear that the addition of PVPh of equal to or more than 20 wt.% into sc-PLA starts to influence the crystalline morphology of sc-PLA to display such a composite ring-banded/ringless spherulite pattern. Less amount of PVPh (< 20 wt.%) in the blends does not show any effect on the stereocomplex morphology.

Figure 4 shows POM and OM images of whole spherulite of sc-PLA/PVPh (70/30) at T_c=170°C (a), the AFM height image of ring-banded pattern (b), and AFM height profile of some parts in ring-banded pattern as indicated by yellow-dashed line (c). The OM image in Figure 4(a) clearly shows that the spherulite morphology is composed of ring-banded pattern in the center and non-banded pattern in the outer region of the center. The AFM height image in Figure 4(b) displays in detail the ring-banded pattern in the center of the spherulite. It clearly shows that the bright and dark regions corresponded to the ridge and valley regions, respectively. The AFM height profile quantitatively shows the height of ridge and valley region in the ring-banded pattern. The distance between two ridges is around 15-20 μm, and the height difference of the highest ridge is around 350 nm from the valley. The AFM height image in Figure 4(b) also shows there is an intermediate ridge between the high ridge and valley. The AFM height profile shows that the intermediate ridge is lower than the high ridge. The height of lower intermediate ridge is around 200 nm – about half height of the high ridge (350 nm). Thus, each band is composed of three hierarchical lamellae of high ridge-half ridge-valley, and this is repeated from the banded core until transition into ringless regions.

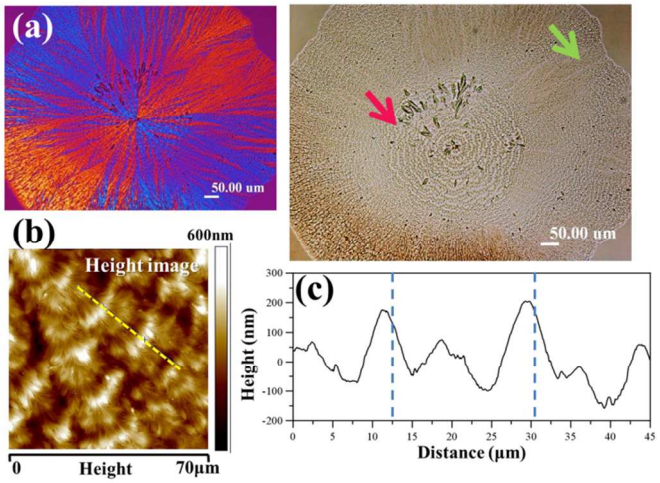

Figure 4. (a) POM and OM images of whole spherulite of sc-PLA/PVPh (70/30) at T_c=170°C, (b) AFM height image of ring-banded core-region, and (c) height profile along yellow-dashed line of image-b.

Detailed lamellar arrangement by AFM

The AFM tapping-phase characterization was carried out to observe the detailed lamellar assembly in three different regions (high ridge, intermediate ridge, and valley) of each band in the ring-banded core of the blend morphology. **Figure 5** shows the phase images of three regions (high ridge, int. ridge, and valley) as indicated by squares in the AFM height image. The lamellae

in the high ridge, low ridge and valley regions are composed of mainly edge-on lamellae. That is, all these regions in each band are composed of same lamellae pattern of no twists or re-orientation, even though three regions have different height profiles that are responsible for the ring-banded pattern in the core of the composite spherulites. AFM graphs clearly demonstrate that the ring-banded pattern in the core of composite spherulite is not caused by gradually twisting or spiraling lamellae from edge-on to flat-on. In some polymers, the ring bands in banded spherulite take vivid birefringence colour contrasts, such as crystallized poly(butylene adipate) (PBA)[23] or poly(ethylene adipate) (PEA).[24] In those cases, the ridge part of PBA or PEA is composed of lamellae of orientations differing significantly from lamellae in the valley. For another example of poly(3-hydroxybutyrate-co-3-hydroxyvalerate) (PHBV),[25] there has been proposal of twisting lamellae based on observations and analyses on crystallized thin films of PHBV. But the vivid birefringence contrast of ring bands have been also claimed to be due to lamellae being radially (in valley) and longitudinally (in ridge) oriented in interior dissection into bulk 3D spherulites.[26] In this present study on sc-PLA/PVPh, the bands in the core region are dramatically different from those bands with birefringence contrasts in PBA, PEA or PHBV, etc. That is, the ridge band is not single, but double-peaks with high- and intermediate-ridges. Both intermediate and high ridges in composite sc-PLA/PVPh spherulite are packed by all edge-on lamellae; and furthermore, even the valley lamellae are also fibrous edge-on, similar to those in the high ridge or intermediate ridge. In the double ridges (high and intermediate), the arrangement of edge-on lamellae is less tidy and more fan out, with more space, in comparison to that in valley part, in which the lamellae are collectively bent into a concave 'V"-shape and become more compact in the limited space. Lamellae in radial growth are not single-stalk crystal plates, as many early investigators so claimed in proposing twist or spiral monotonously for providing ground of bands. Crystal lamellae, by nature, branch out as they grow outward from the center, regardless twist, spiral, or not; however, they cannot remain as single-stalk plate-like crystals as these melt-crystallized lamellae are polycrystalline with branches and not single crystals at all. These AFM graphs on sc-PLA/PVPh reveal clearly and amply demonstrate that most lamellae in the ridge region spray out lamellae branches and these branches bend in either right or left orientation with minor angles, with respect to the original stalks. The fibrous edge-on lamellae even bend in the vertical direction along the radial growth to form periodical ridges and valley in the core banded region of the spherulites.

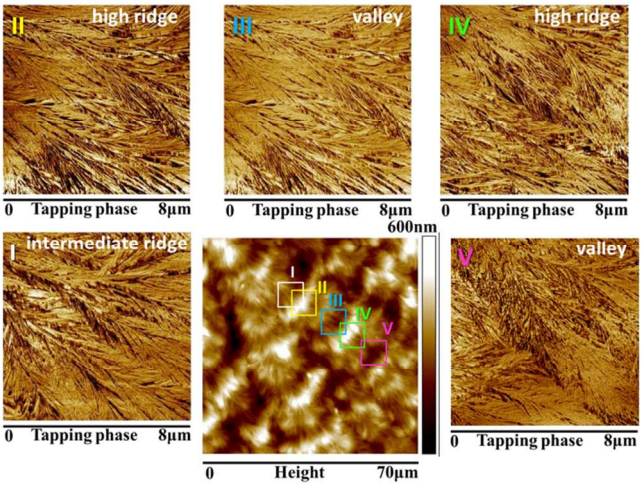

Figure 5. The AFM phase images of three regions (high ridge, low ridge, and valley) in ring-banded pattern of the sc-PLA/PVPh (70/30) blend morphology at T_c=170°C, as indicated by squares in the AFM height image.

As mentioned in previous discussion, the morphology of sc-PLA/PVPh (70/30) blend shows ring-banded pattern in the center and non-banded pattern in the outer region of the spherulite center. **Figure 6** shows the scheme of whole composite spherulite and the detailed lamellar arrangement in four different regions: (I) ridge, (II) valley in central banded core, in comparison to (III) lamellar bundles and (IV) inter-lamellar junction in non-banded outer peripheral region of the spherulite. The ridge and valley regions both are composed of edge-on lamellae as discussed in detail previously. The non-banded region consists of lamellar bundles and inter-lamellar junction as illustrated in the scheme in Fig. 6. Interestingly, the non-banded region is also arranged by edge-on lamellae, either in lamellar bundles or inter-lamellar junction part. So, both ring-banded and non-banded regions are composed of same lamellar pattern which is edge-on lamellae. The arrangement of edge-on lamellae in lamellar bundles part is slightly different with that in junction inter-lamellar part. In the peripheral part, some edge-on lamellae are arranged in radial direction and the others are in tangential direction, as shown by green and yellow arrows. In contrast, the arrangement of edge-on lamellae in the junction inter-lamellar region [Region-IV in outer peripheral of the spherulite] is along radial direction with slightly bending to right and left orientation, as shown in supporting Figure S3. From the observation of the detailed lamellae patterns in core vs. peripheral of spherulites, it is more curious to know the mechanism of such morphology formation. The mechanism will be proposed in the next discussion after the SEM and kinetic observation in the following section.

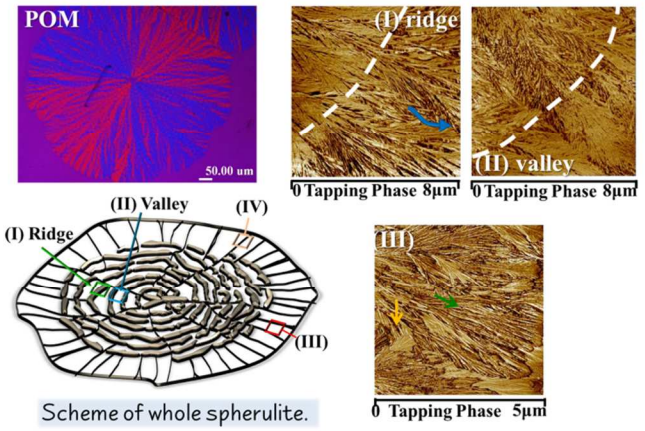

Figure 6. POM, AFM micrographs and scheme of whole spherulite. (I) ridge, (II) valley in banded core, in comparison to (III) lamellar bundles and (IV) inter-lamellar junction in non-banded peripheral region of the spherulite.

Figure 7 displays SEM images of surface of the spherulite, which consists of ring-banded pattern in the center (a) and non-banded pattern in the edge of spherulite (b). The morphology of ring-banded and non-banded patterns is similar, as already explored from AFM images in previous discussion. Figure 7(a) shows a wavy texture on the top surface of ring-banded central core region of the composite spherulite. However, by contrast, a straight fibrous texture is pronounced on the top surface of non-banded pattern in the outskirt region of the spherulite, as shown in Figure 7(b). The AFM and SEM characterizations both show that the lamellar arrangement in ring-banded and non-banded patterns is similar, but the top surface textures are different between the core and outskirt regions of the spherulite. Such patterns occur only after the addition of a certain amount of PVPh to sc-PLA. The inclusion of PVPh should be the main factor for the formation of the wavy texture in the ring-banded core in the sc-PLA spherulites.

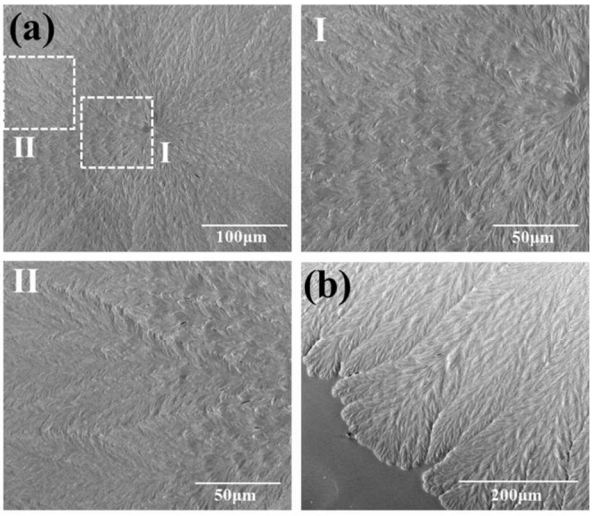

Figure 7. SEM images of composite banded/non-banded spherulites (a) ring-banded pattern in the center, (b) and non-banded pattern in the edge of composite spherulite.

Spherulitic growth rate

Before evaluating the effect of PVPh for the formation of ring-banded pattern, the kinetic observation was necessarily carried out to measure the spherulitic growth rate of the sc-PLA spherulite in the presence of amorphous PVPh as a diluent. **Figure 8** shows the change of radius as function of time for ring-band and non-band region (a) and in situ observation of crystal growth with increasing of time (b). The growth rate of ring-banded pattern is higher than that of non-banded pattern. It is supposed that in the early growth, the crystals grow faster, leading to the formation of ring-banded pattern. After that, the crystals grow more slowly than the previous growth, resulting in the non-banded pattern formation. The existence of amorphous PVPh might influence the kinetic behavior of the spherulites.

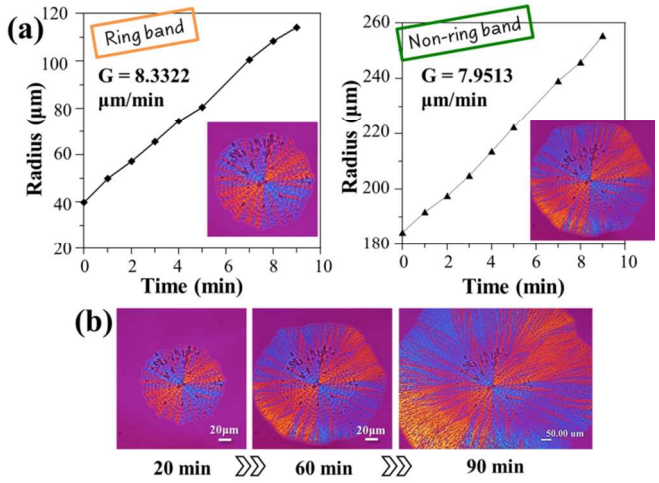

Figure 8. (a) Graph of crystal radius vs. crystallization time of sc-PLA/PVPh (70/30) melt-crystallized at T_c=170°C. (b) In-situ POM images displaying the detailed growth process of unique spherulite.

Proposed mechanism of special spherulites formation

Figure 9 shows a mechanism illustration of lamellar arrangement inside the ring-banded pattern in crystalline morphology of sc-PLA/PVPh (70/30), which suggests the procedures for crystal formation of banded cores to be followed by crystal plates of non-banded peripheral. After the nucleation, in the early growth, the sc-PLA materials diffuse to the growth front to form edge-on lamellae. During the growth process, the non-crystallizable materials (mainly PVPh) were rejected to the growth front of domains mostly underneath the sc-PLA crystals. It is well known that PVPh, with –OH group, has better interaction with the glass substrate than does sc-PLA, so PVPh chains would prefer to go more closely to the glass substrate. Meanwhile, although the PVPh was rejected to underneath of sc-PLA lamellae, the PVPh chains also maintain a strong interaction with sc-PLA via hydrogen-bonding interaction. However, PVPh has a hydroxyl group (–OH) which can strongly interact with the carbonyl group (C=O) of PLLA and PDLA via hydrogen-bonding interaction. Figure S4 shows the FTIR spectra of the sc-PLA/PVPh blends with the

molecular interaction between PVPh and sc-PLA. With increasing sc-PLA contents in the blend, the intensity of the IR peak of self-bounding −OH decreases, showing a corresponding increase in strength of intermolecular hydrogen bonding between PVPh and sc-PLA. The interaction between PVPh and glass substrate and sc-PLA, simultaneously induces the wavy texture (ring-band) in sc-PLA morphology. The non-banded region appears after the complete formation of the ring-banded region in the core. The slower growth rate of this non-banded region causes more diffuse PVPh in sc-PLA lamellae leading to the formation of non-banded pattern.

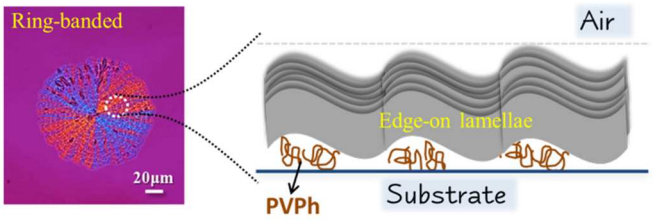

Figure 9. Illustrative mechanism of lamellar arrangement inside the ring-banded core in crystalline spherulite of sc-PLA/PVPh (70/30) melt-crystallized at T_c=170 °C.

Additionally, it should be emphatically pointed out that this special morphology (banded central core in transition to non-banded outer shell) could be found only in a specific condition, such as amorphous PVPh content in the blends being more than 20 wt.% and at fixed range of T_c (160-180°C), suggesting that favourable kinetics might be a governing factor. For the sc-PLA/PVPh (70/30) blend, the composite core-shell ringed/ringless morphology was observed in the blend sample which had been melted for 1 min (t_{max}) at T_{max}=240°C before quenching to T_c. By varying the t_{max}, the blend of sc-PLA/PVPh (70/30) did not show ring-banded and non-banded morphology at all. Supporting information in Figure S5 shows the crystal pattern of sc-PLA/PVPh (70/30) blend at T_c=170°C and various t_{max}. The crystalline pattern of the blend shows dendritic pattern (flower-like pattern in OM image) at melting time (t_{max}) longer than 1 min.

Conclusions

Introduction of amorphous PVPh (20-30 wt.%) into sc-PLA (1:1 equi-molar mixture of LM_w-PLLA and PDLA) was used as a model for investigating effects of strong inter-molecular interactions on the morphology of originally stabilized and stereo-complexed sc-PLA crystals. The ternary blend was first proven to be a miscible mixture as sc-PLA was blended up to 50 wt.% of PVPh. A composite spherulite morphology (core-shell), being composed of ring-banded pattern in the center region gradually transforming into a non-banded pattern in the outer region, was found in sc-PLA/PVPh blends (70/30) melt-crystallized at specific range of T_c (160-180°C). Such unique morphology was only observed when the amorphous PVPh content in the blends was more than 20 wt.%, suggesting that dilution at a critical amount of strongly-interacting and amorphous PVPh is a pre-requisite for re-assembly of originally stabilized sc-PLA spherulites. This composite (core-shell) crystal morphology is distinctly different from that of the crystallized neat sc-PLA (no PVPh), which is a Maltese-cross ringless pattern without ring bands anywhere in the spherulites.

In the composite spherulites of sc-PLA/PVPh blend, both regions of ring-banded and non-banded crystals are composed of edge-on lamellae, but the central-core lamellae undergo periodical waving up and down. AFM analyses reveal that each of the bands is actually composed of two ridges and two valleys – i.e., there is an intermediate ridge between the high ridge and valley. AFM height profile shows that the intermediate ridge is lower than the high ridge. The unique pattern in the banded core of crystallized sc-PLA/PVPh blend is very different from the conventional single ridge-valley band normally seen in other crystallized polymers. Each band in the central core is composed of two ridges and two valleys, and the height of the lower intermediate ridge is around 200 nm – about half height of the high ridge (350 nm). Thus, each band in the central core of spherulites is composed of three hierarchical lamellae of high ridge-half valley-half ridge-valley, and this lamellar assembly is repeated from the banded core until transition into ringless regions. The inter-band spacing between two high ridges is about 15-20 μm. As all lamellae in hierarchical assembly of high ridge-half valley-half ridge-valley are edge-on and pointing radially, there is no optical birefringence contrast between ridges and valley, except for topological up-and-down profiles. The specific stage-wise and preferential interactions between PVPh and sc-PLA and glass substrate, which simultaneously occur during amorphous PVPh rejection and growth process, were evaluated as the reason for the special composite crystal morphology of sc-PLA.

Acknowledgements

This work has been financially supported by a basic research grant (NSC-99-2221-E-006-014-MY3) for three consecutive years from Taiwan's National Science Council (NSC) – now Ministry of Science and Technology (MOST), to which the authors express their gratitude. This research was also partially supported by the Ministry of Education, Taiwan, R.O.C., through the Aim for the Top University Project to the National Cheng Kung University (NCKU).

Notes and references

[a] Department of Chemical Engineering, National Cheng Kung University, Tainan, 701, Taiwan.
[b] Department of Chemical Engineering, Faculty of Industrial Technology, Sepuluh Nopember Institute of Technology, Kampus ITS Sukolilo, Surabaya, East Java 60111, Indonesia.
*Author to whom correspondence should be addressed: emwoo@mail.ncku.edu.tw

Electronic Supplementary Information (ESI) available: [The crystalline morphology of sc-PLA/PVPh (95/5), (90/10), and (80/20) blends at various T_cs. AFM micrograph of inter-lamellar junction in non-banded region. The FTIR spectra of sc-PLA/PVPh at various blend compositions. The crystalline morphology of sc-PLA/PVPh (70/30) blend at T_c=170°C and various t_{max}.]. See DOI: 10.1039/b000000x/

1 Y. Ikada, K. Jamshidi, H. Tsuji and S. H. Hyon, *Macromolecules* 1987, **20**, 904. DOI: 10.1021/ma00170a034
2 T. Okihara, M. Tsuji, A. Kawaguchi, K. I. Katayama, H. Tsuji, S. H. Hyon and Y. Ikada, *J. Macromol. Sci., Phys.* 1991, **B30**, 119. DOI:10.1080/00222349108245788
3 D. Brizzolara, H. J. Cantow, K. Diederichs, E. Keller and A. J. Domb, *Macromolecules* 1996, **29**, 191. DOI: 10.1021/ma951144e
4 H. Tsuji and Y. Tezuka, *Biomacromolecules* 2004, **5**, 1181. DOI: 10.1021/bm049835i
5 H. Tsuji and Y. Ikada, *Macromolecules* 1993, **26**, 6918. DOI: 10.1021/ma00077a032
6 H. Tsuji, S. H. Hyon and Y. Ikada, *Macromolecules* 1991, **24**, 5657. DOI: 10.1021/ma00020a027
7 G. Kister, G. Gassanas and M. Vert, *Polymer* 1998, **39**, 267. DOI: 10.1016/S0032-3861(97)00229-2
8 S. Kang, S. L. Hsu, H. D. Stidham, P. B. Smith, M. A. Leugers and X. Yang, *Macromolecules* 2001, **34**, 4542. DOI: 10.1021/ma0016026
9 L. Cartier, T. Okihara and B. Lotz, *Macromolecules* 1997, **30**, 6313. DOI: 10.1021/ma9707998
10 H. Tsuji, Y. Ikada, S. H. Hyon, Y. Kimura and T. Kitao, *J. Appl. Polym. Sci*. 1994, **51**, 337. DOI: 10.1002/app.1994.070510216
11 S. Brochu, R. E. Prudhomme, I. Barakat and R. Jerome, *Macromolecules* 1995, **28**, 5230. DOI: 10.1021/ma00119a010
12 S. Nurkhamidah and E. M. Woo, *Ind. Eng. Chem. Res.* 2011, **50**, 4494–4503. DOI:10.1021/ie1024547.
13 Y. T. Hsieh, S. Nurkhamidah and E. M. Woo, *Polym. J.* 2011, 43, 762. DOI:10.1038/pj.2011.63.
14 L. T. Lee, E. M. Woo and Y. T. Hsieh, *Polymer* 2012, **53**, 5313. DOI: 10.1016/j.polymer.2012.09.024
15 G. Sun, L. T. Weng, J. M. Schultz and C. M. Chan, *Polymer* 2014, 55, 1829. DOI: 10.1016/j.polymer.2014.02.036
16 E. M. Woo, T. K. Mandal and S. C. Lee, *Colloid Polym. Sci*. 2000, **278**, 1032. DOI: 10.1007/s003960000355
17 D. Maillard and R. E. Prud'homme, *Macromolecules* 2008, 41, 1705. DOI: 10.1021/ma071306u
18 L. Chang and E. M. Woo, *Polymer* 2011, **52**, 68. DOI:10.1016/j.polymer.2010.11.028
19 Y. Li, C. Han, X. Zhang, Q. Dong and L. Dong, *Thermochimica Acta* 2013, **573**, 193. DOI: 10.1016/j.tca.2013.09.035
20 C. Samuel, J. Cayuela, I. Barakat, A. J. Müller, J. M. Raquez and P. Dubois, *ACS Appl. Mater. Interfaces* 2013, **5**, 11797. DOI: 10.1021/am403443m
21 S. H. Li and E. M. Woo, *Polym. J.* 2009, **41**, 374. DOI:10.1295/polymj.PJ2008198
22 S. Nurkhamidah and E. M. Woo, *Macromol. Chem. Phys*. 2013, **214**, 2345. DOI: 10.1002/macp.201300380
23 A. Frömsdorf, E. M. Woo, L. T. Lee, Y. F. Chen and S. Förster, *Macromol. Rapid Commun.* 2008, **29**, 1322. DOI: 10.1002/marc.200800246
24 E. M. Woo, L. Y. Wang and S. Nurkhamidah, *Macromolecules* 2012, **45**, 1375. DOI: 10.1021/ma202222e
25 Z. Wang, Y. Li, J. Yang, Q. Gou, Y. Wu, X. Wu, P. Liu and Q. Gu, *Macromolecules* 2010, **43**, 4441. DOI: 10.1021/ma902773u
26 L. Chang, Y. H. Chou and E. M. Woo, *Colloid Polym. Sci.* 2011, **289**, 199. DOI: 10.1007/s00396-010-2330-7

TOC

Composite ring-banded core and non-banded outer peripheral patterns were found in sc-PLA interacting with amorphous PVPh at several T_cs.